Directional Protective Relaying Based on Amplitude Comparison of Traveling Wave on Continuous Co-phase AT Power Supply System by Using VMD

Shilong Chen[1] *Xiaonan Yang*[1] *Yaoxi Jiang*[2] *Sihong Zhao*[1]

1. College of Electrical Engineering, Kunming University of Science and Technology, China
2. College of Information Engineering and Automation, Kunming University of Science and Technology, China

Abstract: Directional protective relaying based on amplitude comparison of traveling wave on continuous co-phase auto-transformer(AT) power transmission system was proposed. Phase-model transformation is used for decoupling transient fault signals and get aerial mode component. The forward and backward traveling wave are obtained by calculating aerial mode component, then the intrinsic mode function(IMF) components can be obtained through Variational Mode Decomposition(VMD), the module maxima are obtained through calculating the IMF components. The fault direction is determined by the ratio of fault components. If two faults relays at the ends of electric traction networks detect a fault to be in the forward direction, the fault occurred in the internal area, the protection would operate properly. The simulation tests indicate that the protection scheme is feasible, and the proposed protection method can discriminate internal faults from external faults under various fault types, and its performances are immune to fault initial angle, ground resistance, etc.

Index Terms: continuous co-phase traction power supply system (CCTPSS), traction electric network, directional protective relaying(DPR) , amplitude comparison of traveling wave, VMD, modulus maximum

1. INTRODUCTION

Electrified railways have many advantages such as high speed, strong carrying capacity and low energy consumption. At present, railway traction power supply mode generally adopts out-phase power supply mode in china. With higher requirements for high-speed and heavy-duty transportation, the power quality caused by traction load (high-speed railway is mainly negative sequence) [1-2] and phase links have caused concerns domestic and overseas[3-4]. Because the existing power supply mode has an electrical phase separation link, which restricts the speed of the train and causes energy loss, the reliability of the traction power supply system is greatly reduced, and the normal operation of the following vehicles under high speed and heavy load conditions is restricted. In order to solve the problem of de-grading and power-off when the train is over-phase, domestic and abroad scientific researchers have put attention on the co-phase power supply technology and carried out many researches in recent years. The rapid development of power electronics technology and related control theories make it possible to use a continuous co-phase power supply method to completely solve the problems of “over-phase” and power quality of high-speed and heavy-duty of electrified railways [5-7].

As an important part of CCTPSS, the traction network feeder protection is very important, and the existing distance protection has been difficult to meet the requirements of the continuous co-phase power supply traction network feeder protection. Compared with the traditional protection based on power frequency electric quantity, traveling wave protection has fast action performance, and also has the advantages of being unaffected by transition resistance, current transformer saturation, system oscillation and long line distribution capacitance

[8]. The CCTPSS is a multi-power bilateral power supply system, which has the characteristics of continuous traction and ring current in the traction network, control function of the AC-DC-AC power flow controller [9-10]. The characteristics of the CCTPSS determine that it is suitable and necessary to apply the traveling wave protective relaying to the traction network feeder. It is of great theoretical and practical significance to study the traveling wave protection principle and protection scheme of the feeder in the continuous co-phase high-speed railway traction network.

In this paper, directional protective relaying(DPR) based on amplitude comparison of traveling wave of the traction network feeder in the continuous co-phase traction AT power supply system is studied. The principle of DPR based on amplitude comparison of traveling wave of the traction network feeder of the continuous co-phase traction AT power supply system is proposed, and the main influencing factors of the traveling wave protective relaying are analyzed and simulated. A large number of simulation experiments show that the continuous co-phase traction AT power supply system traction network feeder DPR based on amplitude comparison of traveling wave is feasible.

2. BASIC PRINCIPLE OF CONTINOUS CO-PHASE AT TRCTION POWER SUPPLY SYSTEM

China's high-speed railway adopts AT power supply mode. Figure 1 is a schematic diagram of the structure of the continuous co-phase traction AT power supply system. The principle of the CCTPSS is as follows: the step-down transformer steps down the three-phase alternating current of power system and inputs it into the AC-DC-AC converter. The converter converts the three-phase AC power into single-phase AC power through rectification and inverter. Finally, the step-up transformer is used to deliver electrical energy to the traction network. A CCTPSS based on the cascade converter adopts a cascaded multi-level voltage structure, which the filter of the outlet of the single-phase side converter and step-up transformer are canceled. In order to complete the protective action, the circuit breaker and related protection equipment should be installed in the traction network. These devices should be installed in all sections. When the fault occurs in this section, the protective action should promptly and accurately disconnect the fault. The circuit breaker of the partition is usually in a closed state, so that the traction network is powered continuously.

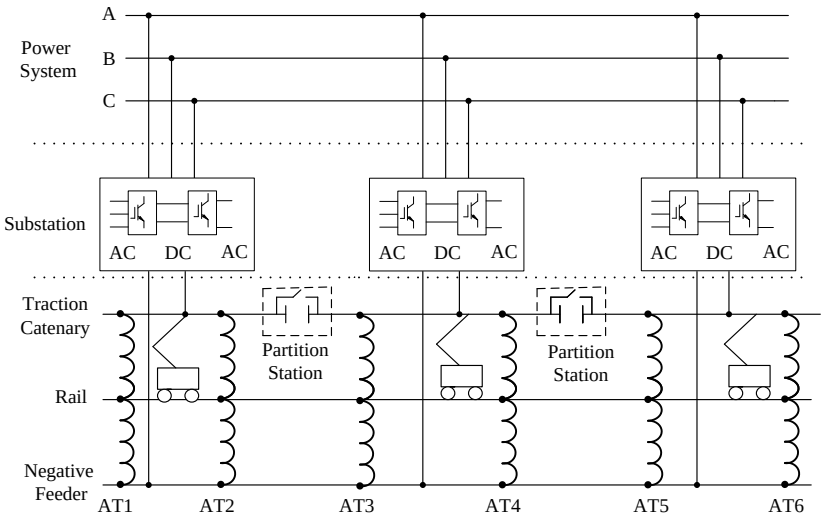

Fig.1 The principle diagram of continuous Co-phase AT traction power supply system

The CCTPSS rectifies the three-phase AC into DC through the power electronic device in the substation, and then converts the DC into single-phase AC. The power system is connected with the traction power supply system through the AC-DC-AC converter, and the power supply network independent of power system is

formed by the conversion and isolation of the DC link, so that the circuit breaker of the partition can be closed, and the traction network can be completely connected. The CCTPSS completely solves the negative sequence and electrical phase separation problems that troubled the electrified railways [5-6].

3. PHASE-MODE TRANSFORMATION

When traveling waves are propagating in a multi-conductor system, there is mutual coupling between the wires, and phase-mode transformation of the traveling waves is required. Phase-mode transformation methods used commonly are: Clark, Karen Bell, symmetrical component method, etc. [8]. In the continuous co-phase traction AT power supply system, two-phase line parameters of traction catenary (C) and the negative feeder (F) are different, and the traction matrix L and the capacitance matrix C of the traction network have the following relationship LC≠CL. It is indicated that the traction network catenary (C) and the negative feed line (F) are non-switching lines, that is, unbalanced lines, and the above methods are not suitable for phase-mode transformation. The fixed transformation matrix cannot be used for the non-switching line. Because the selection of each element of the transformation matrix is related to the line parameters. Therefore, according to the specific line parameters, the numerical simulation method is used to solve the phase transformation matrix. The phase-mode transformation matrix is also frequency dependent, which makes it difficult to apply the phase-mode transformation methods. However, the calculation results show that for the non-switching overhead line, as long as the calculated frequency meets $f \geq 50$ Hz, the transformation matrix is basically independent on the frequency. Therefore, for the electromagnetic transient calculation of the general power system, the phase-mode transformation obtained by numerical calculation without frequency change can be used, and the matrix can still guarantee sufficient calculation accuracy [11]. The transformer matrix T_i for the current and T_u for the voltage of C and F phase,which are calculated by the model traction network parameters used in this paper are as follows [12]:

Current phase-mode transformation matrix:

$$T_i = \begin{bmatrix} 0.8899 & -0.6776 \\ 0.4562 & 0.7354 \end{bmatrix} \tag{1}$$

Voltage phase-mode transformation matrix:

$$T_u = \begin{bmatrix} 0.7632 & -0.4735 \\ 0.7032 & 0.9235 \end{bmatrix} \tag{2}$$

Calculate the modulus components of voltage and current by transforming the matrix:

$$\begin{cases} U = T_u \times U_m \\ I = T_i \times I_m \end{cases} \tag{3}$$

In the formula, U and I are the phase components of the system voltage and current. U_m and I_m are the independent mode components of voltage and current after decoupling.

Deduced from the above formula:

$$\begin{cases} U_m = T_u^{-1} \times U \\ I_m = T_i^{-1} \times I \end{cases} \tag{4}$$

In the formula, T_u^{-1}、T_i^{-1} are the inverse matrix of T_u、T_i respectively.

The voltage and current are decoupled to obtain the ground mode and the aerial mode components. For the ground mode component, the frequency-variation characteristics are obvious, the dispersion is serious, and the attenuation coefficient is larger than the aerial mode component. At the same time, the ground mode wave velocity is greatly affected by the frequency, and is lower than the aerial mode wave velocity. Therefore, the aerial mode component is generally used for the study of traveling wave protection.

4. THE PRINCIPLE OF DPR BASED ON TRAVELING WAVE AMPLITUDE COMPARISON ON CONTINUNOUS CO-PHASE TRACTION AT POWER SUPPLY SYSTEM

The core component of the traveling wave amplitude comparison direction protection [17] is the directional relay, which compares the amplitudes of the reverse traveling wave and the forward traveling wave. From the wave equation, the transient voltage and current at any point on the line can be expressed as:

$$\begin{cases} \Delta u = u_a(t-\dfrac{x}{v}) + u_b(t+\dfrac{x}{v}) \\ \Delta i = \dfrac{1}{Z_c}\left[u_a(t-\dfrac{x}{v}) - u_b(t+\dfrac{x}{v}) \right] \end{cases} \tag{5}$$

Where $v = 1/\sqrt{LC}$ is the propagation velocity of the traveling wave; $Z_C = \sqrt{L/C}$ is the wave impedance of the line; L and C are the inductance and capacitance of the line per unit length; u_a and u_b are the forward wave propagating in the positive direction and the backward wave propagating in the opposite direction of x; Δu and Δi are the fault components of voltage and current.

Equation (5) shows that the transient current and voltage at any point on the line are superposition of the forward and reverse traveling waves. From the equation (5), the forward traveling wave and the reverse traveling wave are respectively:

$$\begin{cases} u_a = (\Delta u + Z_c \Delta i)/2 \\ u_b = (\Delta u - Z_c \Delta i)/2 \end{cases} \tag{6}$$

Where u_a is the forward traveling wave amplitude; u_b is the reverse traveling wave amplitude. $|u_a| \leq |u_b|$, it is a fault in the positive direction; $|u_a| > |u_b|$, it is a fault in the opposite direction.

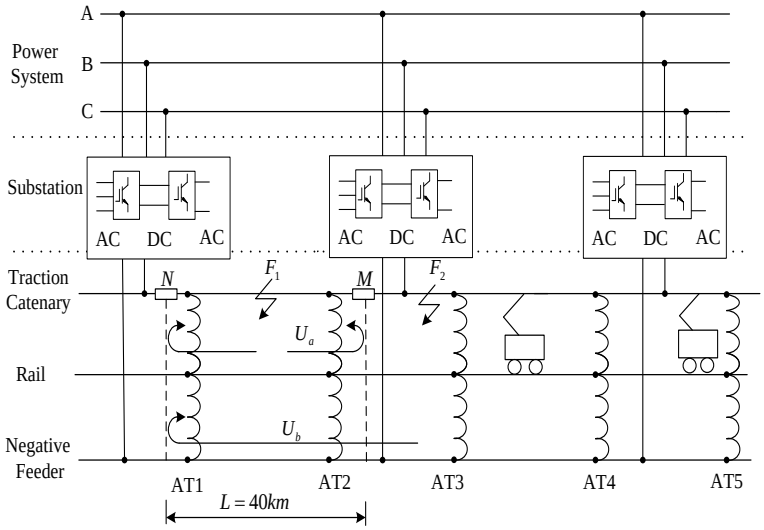

Fig.2 The schematic diagram of DPR based on amplitude comparison of traveling wave on continuous co-phase AT power transmission system

Figure 2 is a schematic diagram of DPR based on amplitude comparison of traveling wave on the continuous co-phase traction AT power supply system, where MN is the protected catenary. The traveling wave flowing from the traction substation to the catenary is a forward traveling wave. When the point F_1 fails, the forward and reverse traveling waves u_a and u_b are detected almost simultaneously on the M side:

$$\begin{cases} u_a = \rho_u U_a \\ u_b = U_a \end{cases} \tag{7}$$

Where ρ_u is the reflection coefficient, U_a is the fault voltage traveling wave signal. Therefore, the amplitude ratio of the forward and reverse traveling waves, $\lambda = u_a / u_b = \rho_u$, is the reflection coefficient of the voltage at the substation.

In this paper, the continuous co-phase traction AT power supply system is adopted. In order to eliminate the influence of the higher harmonics generated by the three-phase/single-phase AC-DC-AC converter on the power quality of the traction network, a capacitor inductor as a filter is installed at the exit of the traction substation, which weaken the traveling wave signal [13]. Since the reflection coefficient ρ_u is around -1, and the amplitude ratio λ is about -1. Therefore, when the fault is positive, $|u_a| \leq |u_b|$.

When a point F_2 fails, the forward traveling wave u_a is first detected on the M side. Since the reverse traveling wave is reflected, the reverse traveling wave u_b is almost 0 at the same time, which is expressed as:

$$\begin{cases} u_a = rU_b \\ u_b = 0 \end{cases} \tag{8}$$

In the formula, r is the refractive coefficient; U_b is the fault voltage traveling wave signal.

In practice, due to the influence of the filtering device of the traction substation, and the error of the value of the wave impedance, the value in the reverse direction of the fault may not be zero, but a small value. That is, the amplitude ratio of the forward and reverse traveling waves, $\lambda >> 1$. In the same positive direction fault, there is also an error in the calculation of the forward traveling wave. Therefore the threshold value can be set to a value greater than 1 by fully considering the influence of the error and the corresponding margin.

Due to the model of the continuous co-phase traction AT power supply system, the amplitude ratio is about 1, considering the sensitivity of the fault protection faults inside and outside the section, the threshold value q in the paper is set to 2.5. From the simulation results later, it can be seen that the threshold value of 2.5 has better sensitivity to faults inside and outside the section.

5. VMD TRAVELING WAVE DETECTION

5.1 VMD principles and algorithm

5.1.1 Principle of VMD

Variational Mode Decomposition is a new signal decomposition method proposed by Dragomiretskiy, etc., in 2014[14]. Compared with the modal aliasing and end-effect in typical decomposition methods such as HHT, VMD decomposes the signal into non-recursive VMD modes, which can realize adaptive segmentation of each component in the signal frequency domain, and the decomposition mode stability is good. VMD also can reflect the singularity of the signal well, effectively overcome the modal aliasing phenomenon, and exhibit better noise robustness and good sampling effect [15-16].

Variation is the essence of for VMD. The algorithm can be transformed into the construction and solution of the variation, which involves three important concepts: classical Wiener filtering, Hibert transform and frequency mixing.

1) Construction of variation

It is assumed that the multi-components signal f is composed of k finite-bandwidth IMF components $u_k(t)$, and the center frequency of each IMF is ω_k, which constraint condition is that the sum of the modal components is equal to the input signal f. The specific construction steps are as follows:

(1) First calculate the correlation analysis signals $u_k(t)$ for each modal by Hibert transform to obtain its unilateral spectrum;

(2) Transfer the spectrum of each modality to the base band based on the hybrid-estimated center frequency $e^{-j\omega_k t}$.

$$\left[\left(\lambda(t)+\frac{j}{\pi t}\right)u_k(t)\right]e^{-j\omega_k t} \tag{9}$$

(3) Calculate the square norm L^2 of the above-mentioned demodulated signal gradient, and estimate the width of each modal signal. The constrained variation is as follows:

$$\begin{cases}\min\limits_{\{u_k\},\{\omega_k\}}\left\{\sum\limits_k\left\|\partial_t\left[\left(\delta(t)+\frac{j}{\pi t}\right)*u_k(t)\right]e^{-j\omega_k t}\right\|_2^2\right\}\\ s.t.\sum\limits_k u_k=f\end{cases} \tag{10}$$

Where: $\{u_k\}$ are the K IMF components obtained from the decomposition, $\{u_k\}:=\{u_1,u_2,\cdots,u_K\}$. $\{\omega_k\}$ are the frequency center of each component, $\{\omega_k\}:=\{\omega_1,\omega_2,\cdots,\omega_K\}$.

2) Solving the variational problem

(1) In order to solve the optimal solution of the above constrained variational problem, the Lagrangian multiplication operator $\lambda(t)$ and the second penalty factor α are introduced to transform the constrained variational problem into a non- constrained variational problem. α guarantee the reconstruction accuracy of the signal, $\lambda(t)$ keep the constraint condition strict. The augmented Lagrangian expression is:

$$L(\{u_k\},\{\omega_k\},\lambda):=\alpha\sum_k\left\|\partial_t\left[\left(\delta(t)+\frac{j}{\pi t}\right)*u_k(t)\right]e^{-j\omega_k t}\right\|_2^2+\left\|f(t)-\sum_k u_k(t)\right\|_2^2+\left\langle\lambda(t),f(t)-\sum_k u_k(t)\right\rangle \tag{11}$$

(2) Solve the above problem by using the alternating directional multiplier method, and continuously update u_k^{n+1}、ω_k^{n+1} and λ_k^{n+1} to obtain the saddle point of the augmented Lagrangian function. The equivalent minimum optimization problem u_k can be expressed as:

$$u_k^{n+1}=\arg\min_{u_k\in X}\left\{\alpha\left\|\partial_t\left[\left(\delta(t)+\frac{j}{\pi t}\right)*u_k(t)\right]e^{-j\omega_k t}\right\|_2^2+\left\|f(t)-\sum_i u_i(t)+\frac{\lambda(t)}{2}\right\|_2^2\right\} \tag{12}$$

(3) Convert it to the frequency domain using Parseval/Plancherel and Fourier equidistant transformation:

$$\hat{u}_k^{n+1}=\arg\min_{\hat{u}_k,u_k\in X}\left\{\alpha\left\|j\omega\left[\left(1+\operatorname{sgn}(\omega+\omega_k)\right)\hat{u}_k(\omega+\omega_k)\right]\right\|_2^2+\left\|\hat{f}(\omega)-\sum_i\hat{u}_i(\omega)+\frac{\hat{\lambda}(\omega)}{2}\right\|_2^2\right\} \tag{13}$$

ω is replaced by $\omega-\omega_k$, the form converted to a non-negative frequency interval integral can be expressed as:

$$\hat{u}_k^{n+1} = \arg\min_{\hat{u},u_k \in X} \left\{ \int_0^{\infty} 4\alpha \left(\omega - \omega_k\right)^2 \left|\hat{u}_k\left(\omega\right)\right|^2 + 2 \left| \hat{f}\left(\omega\right) - \sum_i \hat{u}_i\left(\omega\right) + \frac{\hat{\lambda}\left(\omega\right)}{2} \right|^2 d\omega \right\} \quad (14)$$

The solution to the frequency obtained by quadratic optimization is:

$$\hat{u}_k^{n+1}(\omega) = \frac{\hat{f}(\omega) - \sum_{i \neq k} \hat{u}_i(\omega) + \frac{\hat{\lambda}(\omega)}{2}}{1 + 2\alpha(\omega - \omega_k)} \quad (15)$$

In the same way, the method of updating the center frequency is solved:

$$\omega_k^{n+1} = \frac{\int_0^{\infty} \omega \left|\hat{u}_k(\omega)\right|^2 d\omega}{\int_0^{\infty} \left|\hat{u}_k(\omega)\right|^2 d\omega} \quad (16)$$

In the formula, $\hat{u}_k^{n+1}(\omega)$ is the Wiener filtering of the current residual amount $\hat{f}(\omega) - \sum_{i \neq k} \hat{u}_k(\omega)$; ω_k^{n+1} is the gravity center of the current modal function power spectrum; $u_k(\omega)$ is performed the inverse Fourier transform, and $\{u_k(t)\}$ is the real part.

5.1.2 VMD algorithm

(1) Initialization parameters $\{u_k^1\}, \{\omega_k^1\}, \lambda^1$ and $n = 0$.

(2) $n = n + 1$, start the loop.

(3) Update u_k and ω_k according to equations (15) and (16).

(4) $k = k + 1$, repeat step (3) until $k = K$.

(5) Update λ:

$$\hat{\lambda}^{n+1}(\omega) \leftarrow \hat{\lambda}^n(\omega) + \tau \left[\hat{f}(\omega) - \sum_k \hat{u}_k^{n+1}(\omega) \right] \quad (17)$$

Where τ is the step update coefficient.

(6) Repeat (2) to (5) if

$$\sum_k \frac{\left\| \hat{u}_k^{n+1} - u_k^n \right\|_2^2}{\left\| \hat{u}_k^n \right\|_2^2} < e$$

If $e > 0$, the iteration ends, otherwise return to step (2).

The VMD algorithm is simple, and each mode is continuously updated in the frequency domain, and then is transformed into the time domain by inverse Fourier transform. As the center of the power spectrum of each modality, the center frequency is continuously evaluated and updated in this cycle.

6. COMPARISON OF VMD AND EMD IN SHORT CIRCUIT FAULT

In the paper, VMD is applied to traveling wave fault detection, which provides a reliable basis for traveling wave protection. The data studied are from the negative feeder-rail (F-R) short circuit fault of the continuous co-phase AT traction power supply system. Due to the coupling between the lines, the phase-mode

transformation is first performed for decoupling, and then the VMD and empirical mode decomposition (EMD) are performed. The EMD results are shown in Figure 3. The sampling frequency is 50 kHz, the fault duration is 0.05 s, and the sampling duration is 0.01 s.The fault information is not sufficiently obvious, and there is modal aliasing in the decomposition process. The high-frequency component information in the VMD decomposition result shown in Figure 4 is relatively clear, retaining the intrinsic characteristics of each IMF, reflecting the fault signal changes well, and eliminating the problem of modal aliasing.

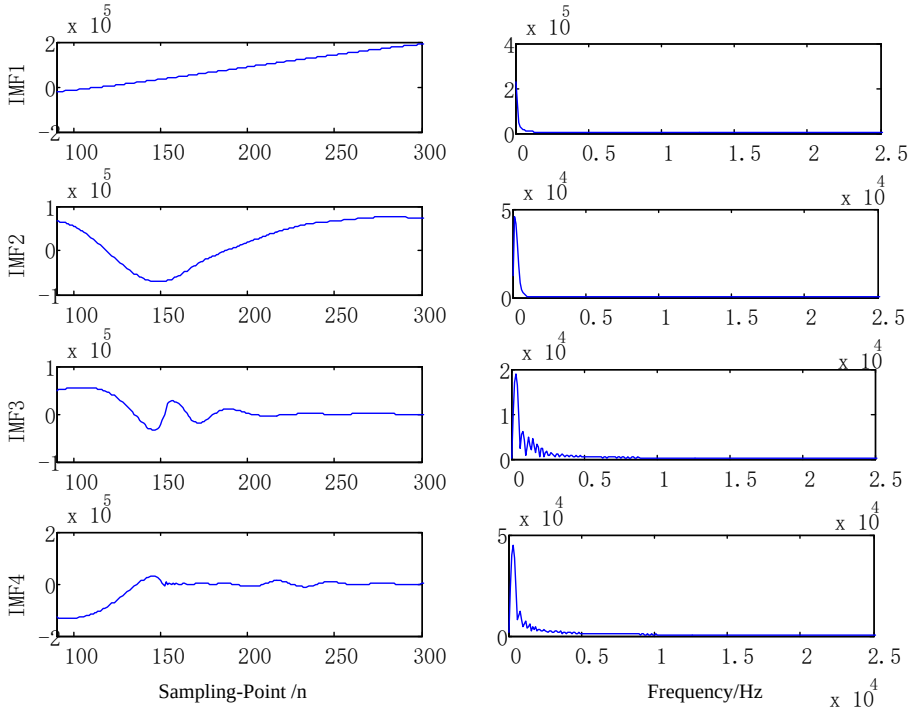

Fig.3 Results of EMD algorithm

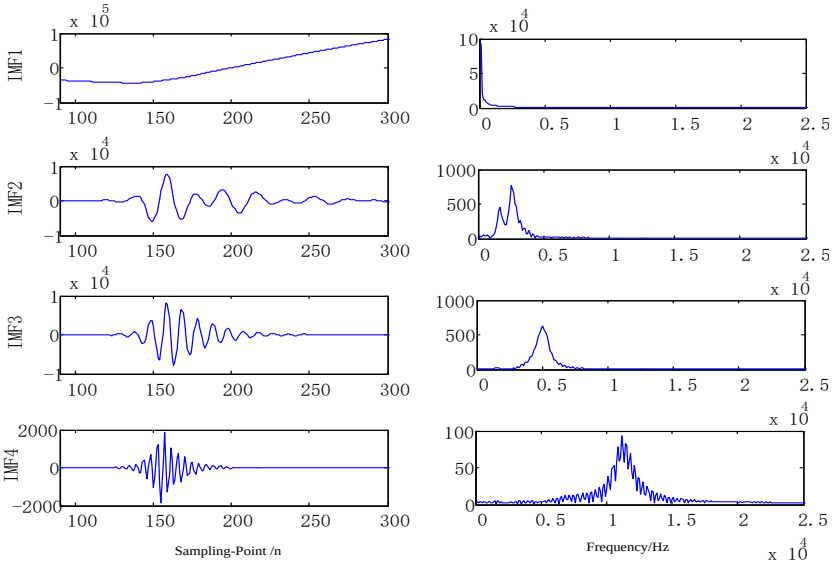

Fig.4 Results of VMD algorithm

The fault information is mainly included in the high-frequency components. It can be seen from the above figure that the IMF fault information corresponding to the frequency center between 1000 and 1500 Hz is relatively clear. Through a large number of simulations, the frequency center of the required component is stable between 800 and 1400 Hz, so the maximum modulus of the IMF is taken from the center of the frequency of

800 to 1400 Hz. For the failure outside of the section on CCTPSS, a filter device composed of a capacitor and an inductor is installed at the exit of the traction substation, which will weaken the traveling wave signal. In order to better extract the high-frequency information, when the VMD decomposition of the subsequent fault simulation is performed, set the number of subsequences $K = 6$, and the penalized parameters $\alpha = 2000$, $\tau = 0$.

7. THE PROCESS OF VMD-BASED DIRECTIONAL PROTECTION BASED ON TRAVELING WAVE AMPLITUDE COMPARISON ON CONTINUOUS CO-PHASE AT TRACTION POWER SUPPLY SYSTEM

In this paper, the VMD can clearly extract the required high-frequency components to realize traveling wave fault detection. Figure 5 is a flow chart [18]. The basic steps are as follows:

(1) Sample and extract fault voltage and current data;

(2) Perform phase-mode transformation on the fault voltage and current signals to obtain a aerial mode components, and calculate a forward traveling wave D_1 and a reverse traveling wave D_2 by the formula;

(3) Perform VMD decomposition on D_1 and D_2 respectively, and take the required IMF component of the corresponding frequencies as fault signals;

(4) Take the modulus maxima of the obtained IMF component as the amplitudes of the forward traveling wave D_1 and the reverse traveling wave D_2;

(5) Judge the section where the fault occurs by comparing the ratio λ of amplitude of D_1 and D_2 with the threshold value q. If both ends λ are smaller than q at the same time, both sides are forward faults, and the fault occurs inside the section, then the protection is performed; otherwise, it is an outside-section fault or no fault, and the protection does not work.

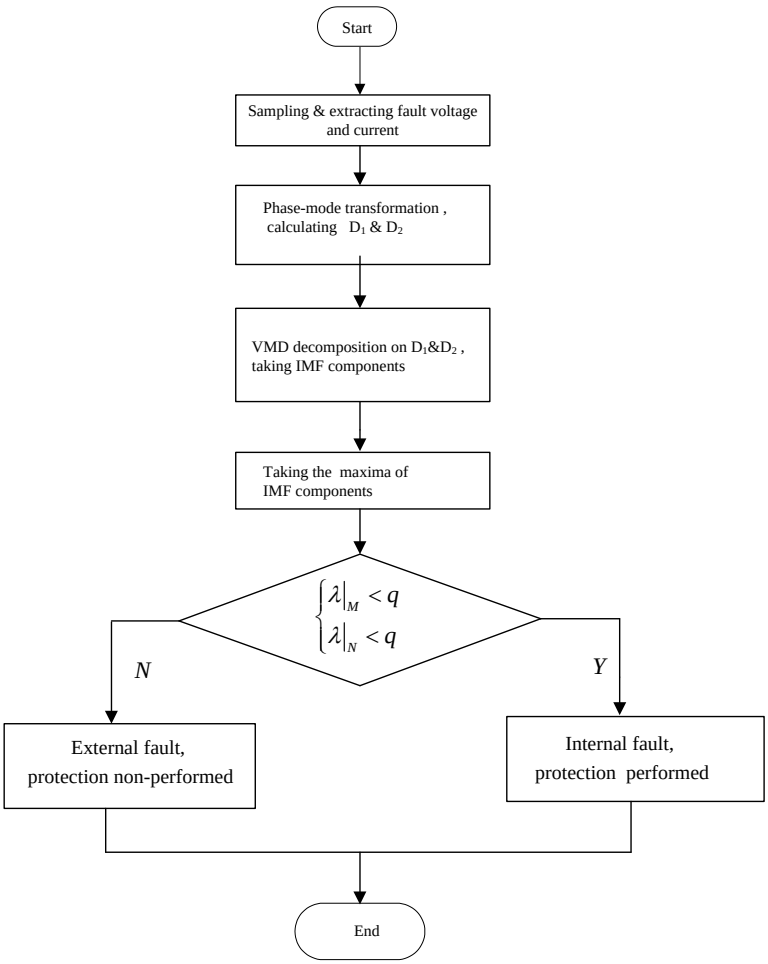

Fig.5 Flowchart for directional protective relaying based on amplitude comparison of traveling wave

8. SIMULATION VERIFICATION

8.1 Simulation Model

In order to verify the correctness of the protection principle, a simulation model of the continuous co-phase traction AT power supply system is established by using PSCAD/EMTDC software, as shown in Figure 2 above. The model is mainly divided into three parts: traction network, AC-DC-AC conversion traction substation and electric locomotive based on CHR2 AC-DC-AC electric locomotive. The traction network consists of catenary, load-bearing cables, positive feeders, rails and feeders connected to the traction substation. In the traction substation, 27.5kV single-phase AC power with equal output amplitude and phase is obtained through rectification and inverter to provide electricity for the locomotive. Traction network short circuit fault is the main fault type in AT power supply mode. The short-circuit fault of the traction network can be subdivided into direct short-circuit and multi-terminal short-circuit. This paper studies the direct short-circuit type. Common short-circuit faults are: Catenary-Rail (C-R) short circuit, Catenary-Feeder l (C-F) short circuit, Feeder -Rail (F-R) short circuit. This paper simulates and analyzes the short-circuit faults and related factors of C-R, C-F and F-R short circuits faults. In the simulation model, the protected catenary is MN, the catenary network length is 40km, and the protection is installed at both ends of the MN catenary. The wave impedance of the aerial mode can be calculated from the catenary net parameters to be 345.234, and the traveling speed of the aerial mode traveling wave is 2.97×10^5 km/ s.

8.2 Typical Faults Simulation

(1) The internal fault

It is assumed that the catenary-rail (C-R) short-circuit fault occurs at the point F_1, which is 25 km away from the M-end. The fault grounding resistance is $50\,\Omega$; the initial angle of the fault is 60°; the sampling frequency is 50 kHz; The threshold value in the paper is set to 2.5; and the test results of the C-R short circuit fault inside MN are shown in Figure 6.

The maximum value ratio $\lambda = |874.659/-778.3897| = 1.124 < k$ of M-terminal can be calculated from the simulation data, so the protection M is judged to be a positive direction failure. Similarly, the maximum value ratio $\lambda = |873.5682/-743.8859| = 1.174 < k$ **of** N-terminal is determined to be a positive direction fault for the protection N. The judgment results of the protection of both terminals of M and N determine that a fault occurs inside the protected catenary, and the protection action occurs immediately.

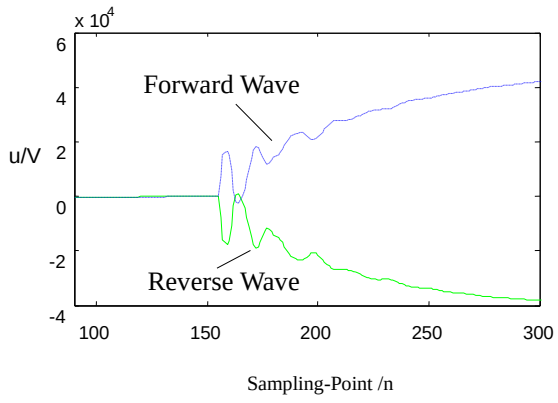

(a) Forward & reverse traveling wave in M-terminal

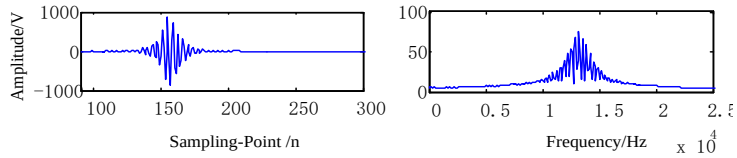

(b) Fault component of forward traveling wave in M-terminal

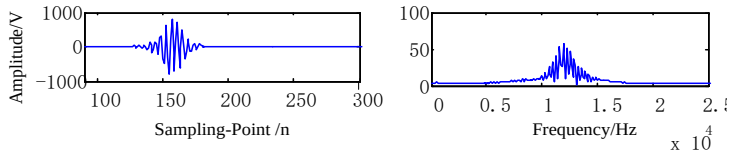

(c) Fault component of reverse traveling wave in M-terminal

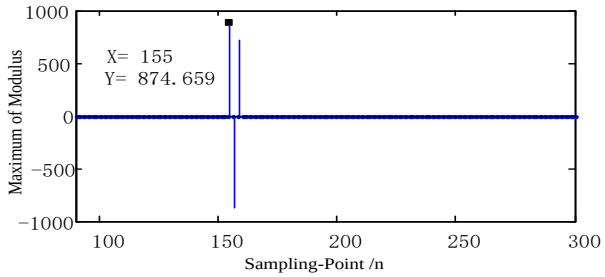

(d) Modulus maxima of forward traveling wave fault component in M-terminal

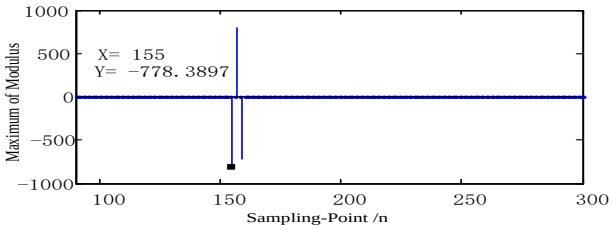

（e）Modulus maxima of reverse traveling wave fault component in M-terminal

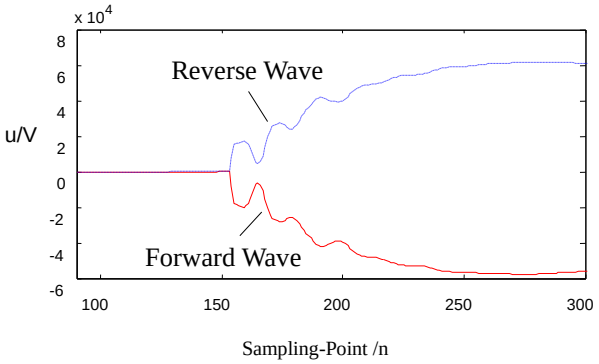

（f）Forward & reverse traveling waves in N-terminal

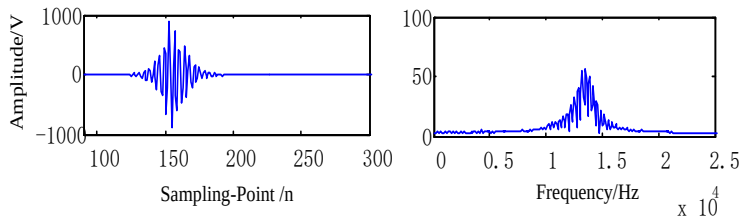

（g）Fault component of forward traveling wave in N-terminal

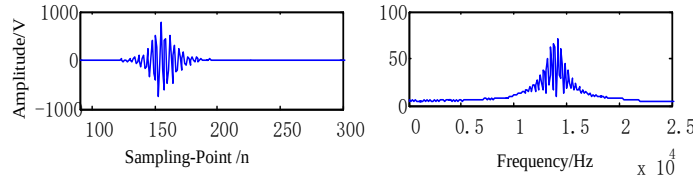

（h）Fault component of reverse traveling wave in N-terminal

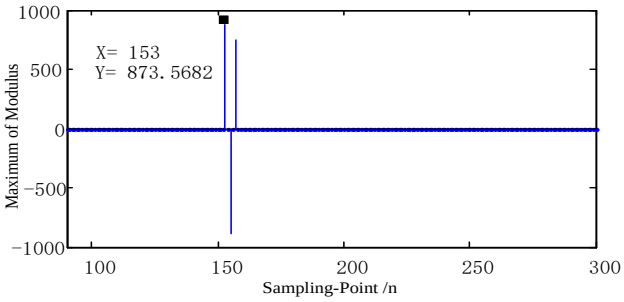

（i）Modulus maxima of forward traveling wave fault component in N-terminal

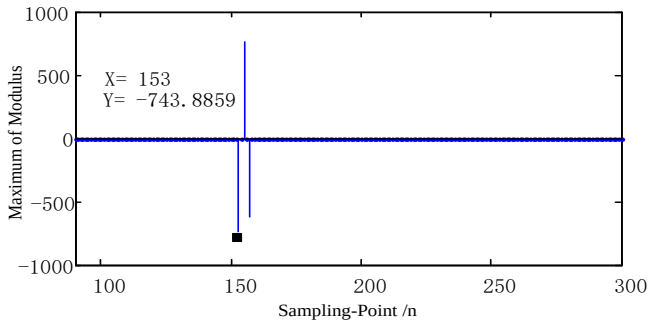

（j）Modulus maxima of reverse traveling wave fault component in N-terminal

Fig.6 The test results of C-R internal short-circuit fault

(2) The external fault

It is assumed that a catenary-rail (C-R) short-circuit fault occurs at a point F_2, which is 15 km away from the M-terminal. The fault grounding resistance is 50 Ω; the initial angle of the fault is 60°; The threshold value in the paper is set to 2.5; and the sampling frequency is 50 kHz. The test results in the C-R short-circuit external fault are shown in Figure 7.

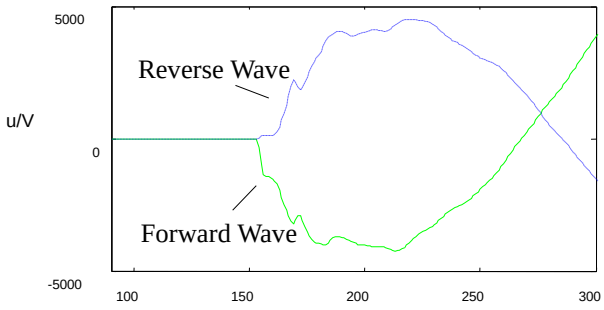

Sampling-Point /n

（a）Forward & reverse traveling waves in M-terminal

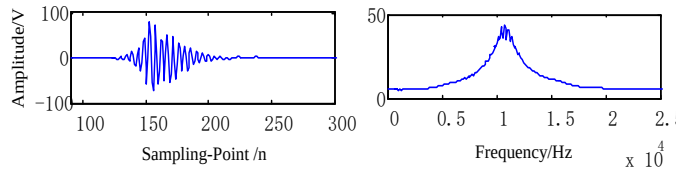

（b）Fault components of forward traveling wave in M-terminal

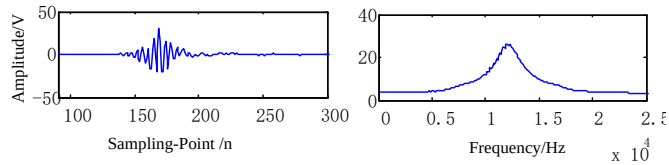

（c）Fault components of reverse traveling wave in M-terminal

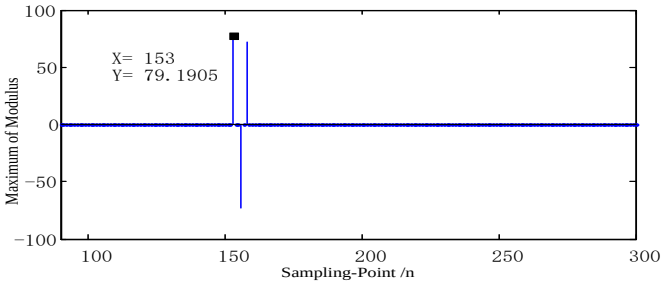

（d）Modulus maxima of forward traveling wave fault component in M-terminal

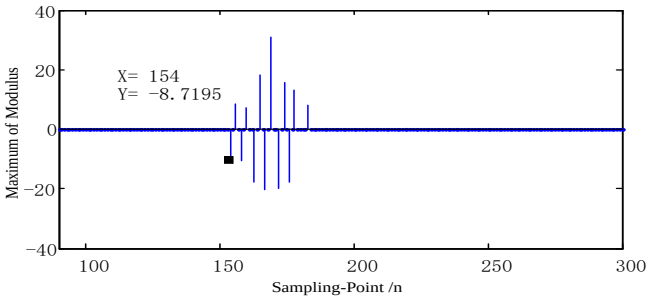

（e）Modulus maxima of reverse traveling wave fault component in M-terminal

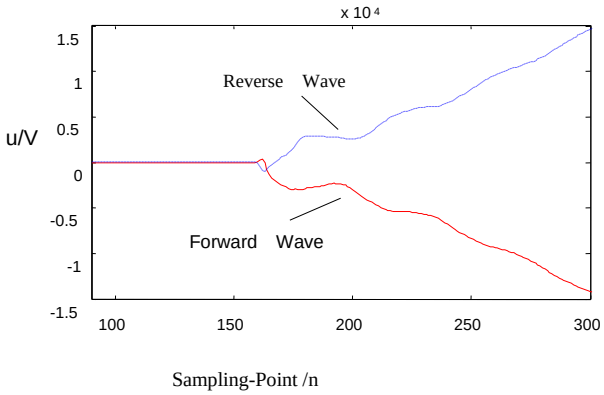

f）Forward & reverse traveling waves in N-terminal

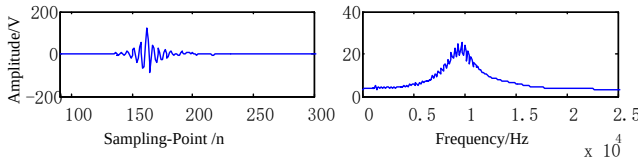

（g）Fault component of forward traveling wave in N-terminal

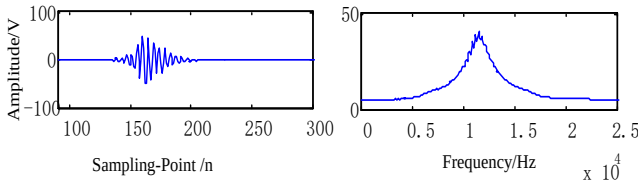

h）Fault component of reverse traveling wave in N-terminal

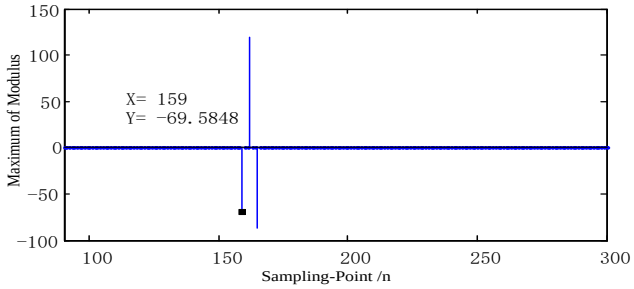

（i）Modulus maxima of forward traveling wave fault component in N-terminal

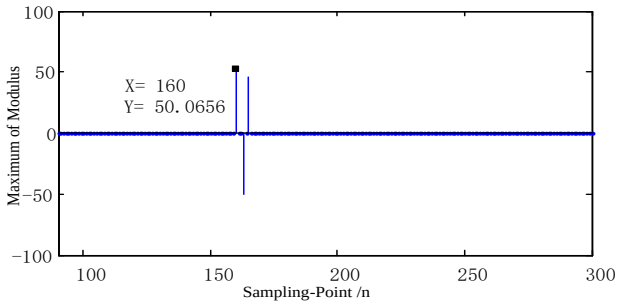

（j）Modulus maxima of reverse traveling wave fault component in N-terminal

Fig.7 The test results of C-R external short-circuit fault

The M-terminal modulus maximum ratio $\lambda = |79.1905/-8.7195| = 9.082 > k$ is calculated from the simulation data, so the protection M is judged to be the reverse direction fault. Similarly, the N-terminal modulus maximum value ratio $\lambda = |-69.5848/50.0656| = 1.390 < k$ is obtained, and the protection N is judged to be a positive direction failure. The results of the protection of both M and N determine that a fault occurs outside the protected catenary section, and the protection does not operate.

8.3 Analysis of factors related to fault

The main factors related to the directional protection based on traveling wave amplitude comparison are: fault types, fault initial angles, fault grounding resistances and so on. The following are simulation results and analysis for different related factors.

(1) Type of fault

For the traction network, the short circuit fault in the traction network is the main type of failure. Common short-circuit faults mainly include catenary-rail (C-R) short circuit, catenary-feeder (T-F) short circuit, feeder-rail (F-R) short circuit. In this paper, the short-circuit faults of C-R, C-F and F-R are simulated. The initial angle is set 90^{o} and the grounding resistance is 0.1Ω. The simulation results for different fault types are shown in Table 1.

Tab.1 Simulation results for different fault types and the performance of relay

Fault point	Type of fault	Location of protection	Modulus maxima of forward wave	Modulus maxima of reverse wave	λ	Direction of fault	result	Protective behavior
F_1	T-F	M	5358.9008	-5381.652	0.996	Forward	Inside Fault	Correct & Action
		N	4585.3338	-4586.3113	0.999	Forward		
	T-R	M	1325.1106	-1252.4031	1.058	Forward	Inside Fault	Correct & Action
		N	1107.3072	-1100.7737	1.006	Forward		
	F-R	M	2543.9175	-2564.69	0.992	Forward	Inside Fault	Correct & Action
		N	1726.3558	-1830.4128	0.943	forward		
F_2	T-R	M	177.8051	-14.0621	12.644	Reverse	Outside Fault	Correct & Non-action
		N	-157.3239	121.7432	1.292	Forward		
	F-R	M	-126.2452	8.8132	14.325	Reverse	Outside Fault	Correct & Non-action
		N	-119.1802	108.9561	1.094	Forward		

The data in Table 1 shows that for various fault types, the protection can make a correct judgment, so the protection is not affected by the types of faults.

(2) Initial angle of fault

The singularity detection is very sensitive to the abrupt signal. Even if the traveling wave component is small at a small angle, the VMD can accurately detect the position of the faulty singular point. When a small angle fault occurs inside MN section, the traveling wave components are small, but the singular performance of the fault first wave head can be detected. When the fault occurs at a small fault angle outside the MN section, considering that the transient signals are attenuated by the capacitor of the traction substation, the fault may not be detected, but the protection can also be correct non-action. When the initial angle of failure is 0, the traveling wave protection does not perform because no transient component appears. This analysis shows that the principle of the directional protective relaying based on the comparison of traveling wave amplitude has a dead zone when the initial angle of failure is zero. In this paper, the different initial angles of the fault are simulated. The fault type is F-R short circuit, the grounding resistance is 0.1Ω, the fault point F_1 is 15km away from the M-terminal inside the MN section, and the fault point F_2 is 15km away from the M-terminal outside the MN section. The initial angle setting and simulation results are shown in Table 2.

Tab.2 Simulation results of different fault initial angles and relay performance

Fault point	Initial angle	Location of protection	Modulus maxima of forward wave	Modulus maxima of reverse wave	λ	Direction of fault	Result	Protective behavior
F_1	3^o	M	225.3549	-246.9066	0.913	Forward	Inside Fault	Correct & Action
		N	170.1608	-177.1504	0.961	Forward		
	10^o	M	509.0666	-495.8147	1.027	Forward	Inside Fault	Correct & Action
		N	422.3924	-382.2658	1.105	Forward		
	60^o	M	2009.5707	-2175.8646	0.924	Forward	Inside Fault	Correct & Action
		N	1626.5047	-1686.6769	0.964	Forward		
F_2	3^o	M	-5.8356	0.69231	8.429	Reverse	Outside Fault	Correct & Non-action
		N	-5.7558	6.9289	0.831	Forward		
	10^o	M	-17.1529	1.3752	12.473	Reverse	Outside Fault	Correct & Non-action
		N	-9.8494	10.0436	0.981	Forward		
	60^o	M	100.9944	-7.9749	12.664	Reverse	Outside Fault	Correct & Non-action
		N	92.8413	-88.5926	1.048	Forward		

The data in Table 2 shows that the protection can be correctly performed for the different initial angle of internal or external faults, so the protection is not affected by the initial angle of the fault.

(3) Grounding resistance

In this paper, the faults of different grounding resistance are simulated, and the fault type is set to C-R short circuit. The initial fault angle is 90^o. The fault point F_1 is 15km away from the M-terminal inside the MN section, and the fault point F_2 is 15km away from the M-terminal outside the MN section. The grounding resistances setting and simulation results are shown in Table 3.

Tab3. Simulation results of different grounding resistances and relay performance

Fault point	Fault resistance (Ω)	Location of protection	Modulus maxima of forward wave	Modulus maxima of reverse wave	λ	Direction of fault	Result	Protective behavior
F_1	10	M	1248.336	-1179.8748	1.058	Forward	Inside Fault	Correct & Action
		N	971.4872	-963.9451	1.008	Forward		
	100	M	901.88	-808.4554	1.116	Forward	Inside Fault	Correct & Action
		N	685.1039	-691.346	0.991	Forward		
	400	M	384.8181	-352.049	1.093	Forward	Inside Fault	Correct & Action
		N	337.5136	-338.3947	0.997	Forward		
F_2	10	M	141.992	-12.4745	11.383	Reverse	Outside Fault	Correct & Non-action
		N	-145.9403	98.4915	1.482	Forward		
	100	M	89.412	-8.9584	9.981	Reverse	Outside Fault	Correct & Non-action
		N	-54.2365	38.5447	1.407	Forward		
	400	M侧	45.8242	-5.4664	8.383	Reverse	Outside Fault	Correct & Non-action
		N侧	-19.283	13.7402	1.403	Forward		

The data in Table 3 shows that as the grounding resistance increases, the amplitudes of the forward and reverse traveling waves at both terminals of the fault line are reduced, but it does not affect the judgment of the faults inside and outside the section, and the judgment result of the principle has no effect. When the grounding resistance outside the section is large and the initial angle is small, the amplitude of the sudden change is weakened, and the modulus maximum value may be smaller than the threshold set in the program, so that the modulus maximum value of the first wave head is not detected. However, when the modulus maximum is not detected, the protection does not operate, so the protection also does not operate correctly.

(4) Location of the fault points

Set the fault type to C-F short circuit, the initial fault angle is 90^{o}, the grounding resistance is 0.1Ω, the fault position setting and simulation results are shown in Table 4.

Tab.4 Simulation results of different fault location and relay performance

Fault point	Fault distance（km）	Location of protection	Modulus maxima of forward wave	Modulus maxima of reverse wave	λ	Direction of fault	Result	Protective behavior
F_1	1	M	-6679.8945	6746.6472	0.990	Forward	Inside Fault	Correct & Action
		N	3815.177	-3842.6116	0.993	Forward		
	10	M	5704.0466	-5712.844	0.998	Forward	Inside Fault	Correct & Action
		N	4131.9233	-4173.9544	0.991	Forward		
	39	M	3739.0221	-3534.0546	1.058	Forward	Inside Fault	Correct & Action
		N	6801.1535	-6819.3362	0.996	Forward		
F_2	1	M	-30.1234	1.8057	16.682	Reverse	Outside Fault	Correct & Non-action
		N	-17.7477	15.2572	1.163	Forward		
	15	M	-21.0575	1.6458	12.795	Reverse	Outside Fault	Correct & Non-action
		N	-16.4831	13.2521	1.244	Forward		
	38	M	-16.5388	1.4647	11.292	Reverse	Outside Fault	Correct & Non-action
		N	-12.4073	12.4081	0.999	Forward		

It can be seen from table 4 that the protection can correctly determine the fault direction at the exit of the catenary. Therefore, the relay performances are not affected by fault locations.

9. CONCLUSION

The traveling wave protection fault detection speed is extremely fast. In this paper, the traveling wave amplitude comparison direction protection is used for the continuous co-phase traction AT power supply system. According to the detailed simulation and analysis of the short circuit fault occurring in the traction network, we got the following conclusions:

(1) Variational mode decomposition (VMD) as a new signal decomposition method, continuously updating the center frequency by variation, effectively avoiding the modal aliasing phenomenon in EMD decomposition, can get better decomposition effect for the required modal components.

(2) VMD-based traveling wave amplitude comparison direction protection can correctly identify various faults in the different traction network location, and is not affected by factors such as fault type, grounding resistance, initial angle of failure, etc.

In summary, the VMD-based traveling wave amplitude comparison type direction protection is suitable for the traction feeder protection of the continuous co-phase traction AT power supply system, and has good engineering application prospects.

Corresponding author:

1.Jiang Yaoxi (jiangyaoxi@kust.edu.cn)

2.Zhao Sihong (zhaosh@kust.edu.cn)

ACKNOWLEDGEMENT

This research was supported by the National Natural Science Foundation of China under Grant 51767012.

REFERENCES

[1] Li Qunzhan. Power Supply Analysis and Comprehensive Compensation Technology of Traction Substation [M]. Beijing: China Railway Publishing House, 2006.

[2] Zhang Xueyuan, Wu Guang-ning, Bian Shanshan, etc. A New Traction Power Grid on Main Railway [J]. Jouranal of the China Railway Society, 2007, 29（3）：100-106.

[3] Guo Yuhua, Lian Jisan, Zhang Kunlun. Influence of Auto Passing of Neutral Section on Electric Locomotive [J]. Electric Drive for Locomotive, 2000, （2）:13-15.

[4] Li Qunzhan. On Some Technical Key Problems in the Development of Traction Power Supply System for High-speed Railway in China [J]. Journal of The China Railway Society, 2010, 32(4):119-124.

[5] Li Qunzhan. On New Generation Traction Power Supply System and Its Key Technologies for Electrification Railway[J]. Journal of Southwest Jiaotong University. 2014, 49（4）:559-568.

[6] Qian Qingquan，Gao Shibin，He Zhengyou，Chen Qizhi，Wu Jiqin. Study of China high-speed railway traction power supply key technology[J].Strategic Study of CAE. 2015,17（4）：9-20.

[7] Shu Zeliang, Xie Shaofeng, Lu Ke, etc. Digital Detection, Control, and Distribution System for Co-phase Traction Power Supply Application [J].IEEE Transactional Industrial. Electronics, 2013,60(5):1832-1839.

[8] Ge Yaozhong. Principles and Techniques of New Relay Protection and Fault Location [M]. Xi'an: Xi'an Jiaotong University Press, 2007.

[9] He Xiaoqiong, Shu Zeliang, Peng Xu, Zhou Qi, Zhou Yingying, Zhou Qijun, Gao Shibin. Advanced Co-Phase Traction Power Supply System Based on Three-Phase to Single-Phase Converter [J].IEEE Transaction on Power Electronics, 2014,29(10):5323-5333.

[10] He Xiaoqiong, Peng Xu, etc. Current-sharing performance of advanced co-phase traction power supply system[J].Electric Power Automation Equipment,2014,34(04):53-58.

[11] Yang Jinyue. Research on traveling wave fault location of AT power supply traction network [D]. East China Jiaotong University, 2013.

[12] Li Jianping. Research on traveling wave propagation characteristics and protection of traction network of contiuous co-phase traction power supply system [D]. Kunming University of Science and Technology, 2017.

[13] Zhao Li. Research on grid-connected control of multi-traction substation based on five-level three-phase to single-phase converter [D]. Southwest Jiaotong University, 2017.

[14] Dragomiretskiy K, ZOSS D. Variational mode decomposition[J]. IEEE Transaction on Signal processing,2014,62(3):531-544.

[15] Yanfeng Gao. Study on Method of Lightning Strike Identification and Fault Location of Transmission Lines Based on Current Traveling Waves[D]. North China Electric Power University，2016.

[16] Gao Yanfeng, Zhu Yongli, Yan Hongyan, Wu Yingjie. Study on Lighting Fault Locating of High-voltage Transmission Lines Based on VMD and TEO[J].Transactions of China Electro technical Society,2016,31(01):24-33.

[17] Dong Xingli, Ge Yaozhong, Dong Xingzhou, etc. Directional protective relaying based on amplitude comparison of travelling wave by using wavelet transform[J]. Automation of Electric Power Systems. 2000(17):11-15.

[18] Zou Guibin, Gao Houlei, Jiang Shi-fang, Xu Bingyin. Novel Transient Travelling Wave Based Amplitude Comparison Ultra High-speed Directional Protection[J]. Proceedings of the CSEE, 2009,29(07):84-90.